The Plant Cell, Vol. 14, 33–46, January 2002, www.plantcell.org © 2002 American Society of Plant Biologists

SGR2, a Phospholipase-Like Protein, and ZIG/SGR4, a SNARE, Are Involved in the Shoot Gravitropism of Arabidopsis

Takehide Kato,[a,1] Miyo Terao Morita,[b,1] Hidehiro Fukaki,[b] Yoshiro Yamauchi,[a] Michiko Uehara,[a] Mitsuru Niihama,[b] and Masao Tasaka[b,2]

[a] Department of Botany, Graduate School of Science, Kyoto University, Sakyo-ku, Kyoto 606-8502, Japan
[b] Graduate School of Biological Sciences, Nara Institute of Science and Technology, Nara 630-0101, Japan

In higher plants, the shoot and the root generally show negative and positive gravitropism, respectively. To elucidate the molecular mechanisms involved in gravitropism, we have isolated many shoot gravitropism mutants in Arabidopsis. The *sgr2* and *zig*/*sgr4* mutants exhibited abnormal gravitropism in both inflorescence stems and hypocotyls. These genes probably are involved in the early step(s) of the gravitropic response. The *sgr2* mutants also had misshapen seed and seedlings, whereas the stem of the *zig*/*sgr4* mutants elongated in a zigzag fashion. The *SGR2* gene encodes a novel protein that may be part of a gene family represented by bovine phosphatidic acid–preferring phospholipase A1 containing a putative transmembrane domain. This gene family has been reported only in eukaryotes. The *ZIG* gene was found to encode AtVTI11, a protein that is homologous with yeast VTI1 and is involved in vesicle transport. Our observations suggest that the two genes may be involved in a vacuolar membrane system that affects shoot gravitropism.

INTRODUCTION

Plants settle in their place of germination through their lifetime and cannot escape the various environmental stimuli to which they are exposed. Consequently, plants have evolved many mechanisms by which they can sense and adapt themselves to various environmental changes. Gravitropism is one of those important environmental responses, particularly for land plants. This is the response that the plant makes when it is laid flat on the ground, namely, the shoot curves up (negative gravitropism) and the root curves down (positive gravitropism). This response is necessary to position the plant so that its leaves face the source of light energy and its roots can take up water and various nutrients.

A number of physiological and cytological studies using many different species of plants have demonstrated that amyloplasts that accumulate starch are involved in gravity perception as statoliths and that auxin is involved in the asymmetric growth between the upper and lower tissue of the responding organ that results in the gravitropic curvature (Sack, 1991; Kaufman et al., 1995). These studies also have suggested that various signal molecules, such as Ca^{2+}, calmodulin, and inositol 1,4,5-triphosphate, and pH change are involved in the signal transduction that generates the gravitropic response (Belyavskaya, 1996; Sinclair and Trewavas, 1997; Perera et al., 1999; Scott and Allen, 1999; Fasano et al., 2001).

To elucidate the molecular mechanism of the gravitropic response in higher plants, many mutants with aberrant root or shoot gravitropism have been isolated from Arabidopsis (Firn et al., 2000; Tasaka et al., 2001). With respect to root or hypocotyl gravitropism, most of the mutants that are abnormal in this function also respond abnormally to auxin treatment. This suggests that a number of auxin-related genes are involved in this response. These include the *AUX1* (*AUXIN RESISTANT 1*) and *EIR1*/*AGR1*/*PIN2* (*ETHYLENE INSENSITIVE ROOT 1*/*AGRAVITROPIC 1*/*PIN-FORMED 2*) genes, which appear to be involved in auxin transport (Bennett et al., 1996; Chen et al., 1998; Luschnig et al., 1998; Müller et al., 1998; Utsuno et al., 1998), as well as the *AXR1* (*AUXIN RESISTANT 1*) gene, which encodes a protein similar to the ubiquitin-activating enzyme E1 (Leyser et al., 1993). Also involved may be the *MSG1*/*NPH4* (*MASSUGU 1*/*NONPHOTOTROPIC HYPOCOTYL 4*; *ARF7*) gene, which is a member of the *ARF* gene family that encodes a putative transcription factor that binds to a specific sequence in the promoter of many auxin-regulated genes (Liscum and Briggs, 1996; Watahiki and Yamamoto, 1997; Harper et al., 2000). Other genes that may belong to the *Aux*/*IAA* gene family include *AXR2* (*IAA7*), *AXR3* (*IAA17*), *SHY2* (*SUPPRESSOR OF HY2*; *IAA3*), *MSG2* (*IAA19*), and *SLR* (*SOLITARY ROOT*; *IAA14*). The expression of these genes is regulated by auxin (Wilson et al., 1990; Timpte et al., 1992; Rouse et al., 1998; Tian and Reed, 1999; Nagpal et al., 2000;

[1] These authors contributed equally to this work.
[2] To whom correspondence should be addressed. E-mail m-tasaka@bs.aist-nara.ac.jp; fax 81-743-72-5489.
Article, publication date, and citation information can be found at www.plantcell.org/cgi/doi/10.1105/tpc.010215.

Fukaki et al., 2002). These results indicate that a signaling pathway(s) dependent on auxin is crucial for gravitropism, probably for the differential growth involved in this response.

Another mutant that shows a reduced gravitropic response in both the root and the hypocotyl is the *rhg* (*root and hypocotyl gravitropism*) mutant, which is allelic to *arg1* (*altered response to gravity*) (Fukaki et al., 1997). The *ARG1* gene encodes a novel protein with a J domain that is conserved in the DnaJ/Hsp40 gene family and with a putative coiled-coil domain that could interact with microtubules or microfilaments (Sedbrook et al., 1999).

With respect to shoot gravitropism, when Arabidopsis inflorescence stems are placed horizontally, they bend upward, and the curvature reaches 90° after ~90 min (Fukaki et al., 1996a). We have isolated a number of *sgr* (*shoot gravitropism*) mutants that are abnormal in this function and have found that at least seven loci are involved (Fukaki et al., 1996b, 1998; Yamauchi et al., 1997). It is believed that the transport and distribution of auxin are involved in both gravitropism and phototropism (Kaufman et al., 1995). Because all of the *sgr* mutants can perform the phototropic response (Fukaki et al., 1996b; Yamauchi et al., 1997), the transport and distribution of auxin probably is normal. Thus, it is more likely that the *sgr* mutants are impaired in either their perception of gravity or the signaling pathway(s) involved in the gravitropic response. The *sgr1* and *sgr7* mutants, which show an agravitropic response in both the hypocotyl and the inflorescence stem, are allelic to the radial pattern mutant of the root, *scr* (*scarecrow*) (Scheres et al., 1995; Di Laurenzio et al., 1996), and *shr* (*short-root*) (Scheres et al., 1995), respectively. Their roots, however, exhibit normal gravitropism. Their primary defect is the absence of a normal endodermal cell layer not only in the root but also in the hypocotyl and inflorescence stem. This indicates that endodermal cells are essential for shoot gravitropism (Fukaki et al., 1998).

The *sgr2* and *zig* (*zigzag*)/*sgr4* mutants are abnormal in the gravitropism of their inflorescence stems and hypocotyls (Fukaki et al., 1996b; Yamauchi et al., 1997). As reported here, we have characterized mutants in detail and have cloned the *SGR2* and *ZIG*/*SGR4* genes. *SGR2* was found to encode a novel protein that is homologous with the phosphatidic acid–preferring phospholipase A1 (PA-PLA1) found in bovine testis (Higgs et al., 1998). In addition, *ZIG*/*SGR4* was found to encode AtVTI11, which was identified by an Arabidopsis expressed sequence tag (EST) database search as being homologous with the yeast v-SNARE VTI1p (Zheng et al., 1999). This finding suggests that membrane traffic is involved in gravitropism.

RESULTS

Gravitropic Responses of *sgr2* and *zig*/*sgr4*

After being placed horizontally, Arabidopsis wild-type (Columbia [Col]) inflorescence stems bent upward, and the curvature reached 90° in ~90 min (Figure 1A). In contrast, the

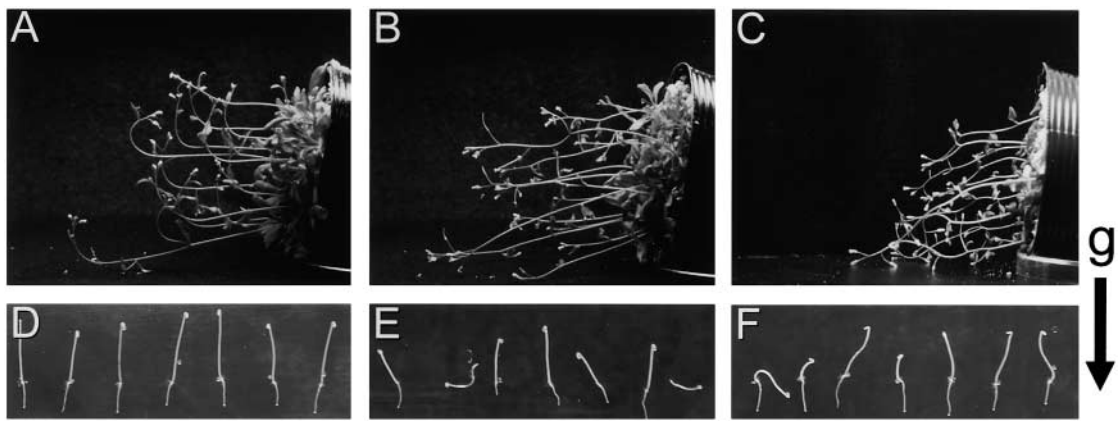

Figure 1. Shoot Gravitropism of *sgr2* and *zig*/*sgr4*.

(A) to **(C)** Gravitropic response of inflorescence stems of 5-week-old plants after 90 min of horizontal gravistimulation.
(A) Wild type (Col).
(B) *sgr2-1*.
(C) *zig-1*.
(D) to **(F)** Gravitropism of 3-day-old etiolated seedlings.
(D) Wild type (Col).
(E) *sgr2-1*.
(F) *zig-1*.
The arrow indicates the direction of gravity (g).

sgr2-1 and *zig-1/sgr4-1* inflorescence stems showed little response (Figures 1B and 1C), as reported previously (Fukaki et al., 1996b; Yamauchi et al., 1997). In addition, etiolated wild-type seedlings grew upward uniformly, whereas those of *sgr2-1* and *zig-1/sgr4-1* did so in a disorderly fashion (Figures 1D to 1F). The roots in both mutants showed normal positive gravitropism (Fukaki et al., 1996b; Yamauchi et al., 1997). Thus, *SGR2* and *ZIG/SGR4* are involved specifically in shoot gravitropism. Apart from their abnormal gravitropic response, the mutants also exhibited some morphological anomalies. In the wild-type plant, primary inflorescence stems grew straight up, as did the lateral shoots (Figure 2A). In *sgr2-1*, however, the inflorescence stems wound slightly at each node and the lateral shoots rolled downward (Figure 2B). In contrast, the inflorescence stems of *zig-1/sgr4-1* elongated in a zigzag fashion, although its lateral shoots tended to curl downward, similar to those of *sgr2-1* (Figure 2C). Because of this characteristic stem shape, *sgr4* was renamed *zigzag*.

The kinetics of the gravitropic response of the inflorescence stems from the mutant plants were measured (Figure 3). In the wild-type plant, the stem segments began to bend upward within 30 min and the curvature reached 90° in ~90 min. After bending too far, they curved in the opposite direction and finally settled at 90° (Figures 3A and 3B) (Fukaki et al., 1996a). Four *sgr2* alleles were newly isolated in addition to the six alleles reported previously (Fukaki et al., 1996b). The gravitropic response of all 10 alleles was measured, which allowed the alleles to be classified into strong (*sgr2-1*, *sgr2-3*), middle (*sgr2-5*, *sgr2-6*), or weak (*sgr2-10*) alleles (Figure 3A and data not shown). The strong alleles showed little gravitropic curvature even after 24 hr, whereas the middle alleles showed some slow gravitropic response, but the curvature did not reach 90° even after 24 hr. The kinetics of response in *sgr2-10*, which has the weakest allele, were comparable to that of the wild type except that its initial response had a lag time and its later response after bending excessively (after 150 min) was slow (Figure 3A, closed squares).

Two additional alleles of *zig* were isolated, both of which had the characteristic zigzag-shaped inflorescence stem (data not shown). The stem segments of *zig-1* and *zig-2* showed little and no response to gravity, respectively, even after 24 hr (Figure 3B). *zig-3*, however, did show a response to gravity, albeit one that was retarded markedly. These plants started to bend upward within 60 min, after which it took 3 hr to reach 90°. After bending excessively, the curvature settled at 90° after 24 hr.

The Seed and Seedling Phenotype of *sgr2*

Because *sgr2* mutations are recessive (Fukaki et al., 1996b), the segregation ratio of F2 plants produced by the crossing of *sgr2* and wild-type plants is expected to be 1:3. However, the incidence of *sgr2* mutants was slightly lower than this

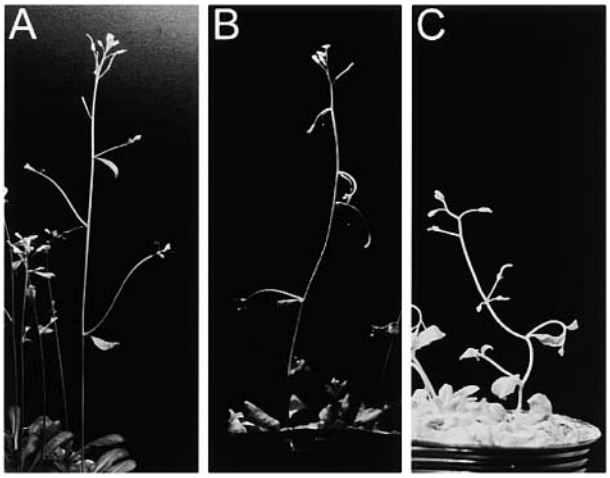

Figure 2. Morphology of Primary and Lateral Shoots.

Aerial parts of wild type (Col) **(A)**, *sgr2-1* **(B)**, and *zig-1* **(C)** plants.

(data not shown). Although all of the wild-type and most of the *sgr2* seed were uniform in their oval shape and size (Figure 4A), some *sgr2* seed were irregular in shape and shrunken (Figure 4C). The shrunken seed did not germinate, which may be responsible for the slight decrease in the incidence of mutant F2 plants. After germination, although most *sgr2* seedlings were normal in shape, some were abnormal (Figures 4B and 4D). For example, some seedlings had three cotyledons (Figure 4D) or only one cotyledon. Some were even more abnormally shaped (data not shown). All of these abnormally shaped seedlings had an active shoot apical meristem, and the gravitropic response of their inflorescence stems was aberrant.

Map-Based Cloning of *SGR2*

We performed map-based cloning of the *SGR2* gene by analyzing ~1700 chromosomes. *SGR2* was found to map 0.8 to 1.0 centimorgan south of m254 on chromosome 1 (Figure 5A). Because *sgr2-8*, *sgr2-9*, and *sgr2-10*, which were mutagenized by fast neutron exposure, were expected to have a deletion in the *SGR2* locus, they were used for DNA gel blot analysis. The 10-kb fragment that included the T7 end of bacterial artificial chromosome T4D9 (Figure 5A, probe X) was used as a probe. The polymorphism between the wild-type and *sgr2-10* genomes was detected after digestion with XbaI (Figure 5B). Thus, *SGR2* is located around the probe X fragment. Approximately 25 kb of the genome that includes the region corresponding to probe X was sequenced (Figure 5A, gray lines). *sgr2-10* was shown to have a 10-kb deletion in the sequenced locus, and the deleted fragment seemed to have translocated into a locus 92-kb south (data not shown). The sequenced locus was predicted

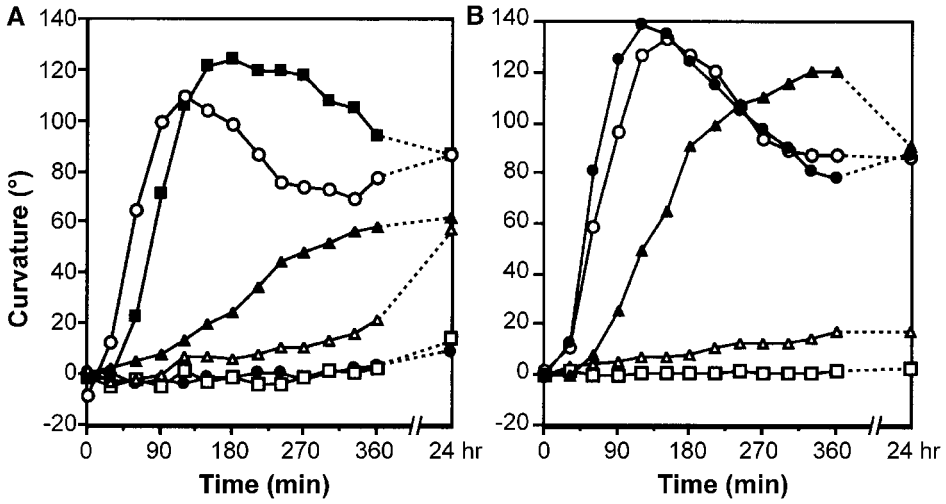

Figure 3. Time Course of the Gravitropic Response of Inflorescence Stems.

(A) The gravitropic response of *sgr2* alleles: wild-type (Col; open circles), *sgr2-1* (closed circles), *sgr2-3* (open squares), *sgr2-5* (closed triangles), *sgr2-6* (open triangles), and *sgr2-10* (closed squares) stem segments.

(B) The gravitropic response of *zig/sgr4* alleles: wild-type (Col; open circles), *zig-1* (open triangles), *zig-2* (open squares), wild-type (Wassilewskija; closed circles), and *zig-3* (closed triangles) stem segments.

Stem segments were gravistimulated by being placed horizontally at 23°C in the dark. The curvature was measured at the times indicated.

to contain more than eight putative coding regions. Finally, the mutations of all *sgr2* alleles were mapped to one gene located just to the south of the *sgr2-10* deletion site (Figure 5A).

The *SGR2* gene was composed of 22 exons and encoded a protein with a molecular mass of 106.3 kD (933 amino acids) (Figure 5C). Both *sgr2-1* and *sgr2-4*, the strong alleles, had the same mutation, namely, a G-to-A transition at the boundary between the 20th exon and the intron. In *sgr2-2* and *sgr2-5*, their respective codons (Arg-358 and Trp-189) had been changed into stop codons by the transition of a single nucleotide (Figure 5C). In both *sgr2-6* and *sgr2-3*, there was a missense mutation that caused the amino acid substitutions of G320S and G446A, respectively. Both Gly residues are highly conserved in the *SGR2* gene family (Figure 6B). Four alleles (*sgr2-7*, *sgr2-8*, *sgr2-9*, and *sgr2-10*) had a deletion in this locus, as shown in Figure 5C.

The ~7.3-kb wild-type genome fragment that extends from 1.2 kb upstream of the putative transcription start site to 400 bp downstream of the putative transcription termination site could complement the shoot gravitropism of *sgr2-1* (Figure 5D). This finding indicates that the gene is identical to *SGR2*. RNA gel blot analysis of the wild-type plant was performed using the 700-bp sequence in the 3′ region of *SGR2* as a probe. An ~3.0-kb transcript of *SGR2* was detected in all organs, even in the root, which does not show an aberrant response to gravity (Figure 5E). *SGR2* mRNA was barely detected in siliques by RNA gel blot analysis but could be detected by nonquantitative reverse transcription–polymerase chain reaction (RT-PCR) (data not shown).

SGR2 Encodes a Protein Homologous with PA-PLA1

SGR2 was found to be a novel and unique gene that does not have a homologous gene in the Arabidopsis genome. In tomato (AW035183, AI486639, AW220938, AW219077, and AW930345), soybean (BE058094 and BE058090), cotton (AW725387), rice (C26667, D43182, and C28346), and maize (AW424734, AW313200, and AW324709), EST clones that are homologous with *SGR2* have been registered in the database, suggesting that *SGR2*-like genes are present in other higher plants. SGR2 also was similar in sequence to proteins from several eukaryotes, such as *Schizosaccharomyces pombe* (genes SPAC20G8.02 and SPCC1020.13), *Saccharomyces cerevisiae* (gene YOR022c), *Neurospora crassa* (gene B14D6.220), *Caenorhabditis elegans* (gene M03A1.6), *Drosophila melanogaster* (gene CG8552), and mammals. Thus, these genes constitute a small gene family. Some regions of the gene were highly conserved within the family, but others were not. The proteins of two of the members of this family have been characterized, namely, PA-PLA1, whose gene was cloned from bovine testis (Higgs et al., 1998), and p125, which was identified in human (Tani et al., 1999). The latter has been cloned as a Sec23p-interacting protein and is suggested to be involved in vesicle transport from the endoplasmic reticulum to the Golgi apparatus (Figures 6A and 6B).

SGR2 bears the lipase consensus sequence (GXSXG) that is highly conserved in all members of the gene family except PA-PLA1 (SHSLG). In *sgr2-3*, an amino acid substitution of

Arg for the last Gly in the consensus sequence caused a comparatively profound inability to respond to gravity (Figures 3A and 6B). This finding suggests that the lipase consensus sequence is important in gravitropism. SGR2 also was predicted by the TMpred program (http://www.ch.embnet.org/software/TMPRED_form.html; Hofmann and Stoffel, 1993) to bear a transmembrane domain at residues 669 to 689. This region also is conserved among the various members of the PA-PLA1 gene family and shows sequence similarity to one of the putative transmembrane domains of the retinal degeneration B protein. This protein is an integral membrane protein (Vihtelic et al., 1991, 1993), which suggests that the members of the PA-PLA1 gene family code for membrane proteins. Another feature of SGR2 was a coiled-coil structure predicted at residues 593 to 635 by the COILS program (http://www.ch.embnet.org/software/COILS_form.html; Lupas et al., 1991). This structure was found in PA-PLA1 (residues 580 to 606) and MO3A1.6 (residues 445 to 481) (Higgs et al., 1998). These predicted coiled-coil domains are located at similar positions between the lipase consensus sequence and the putative transmembrane domain in each of these three proteins, although there is no amino acid sequence similarity (Figure 6A).

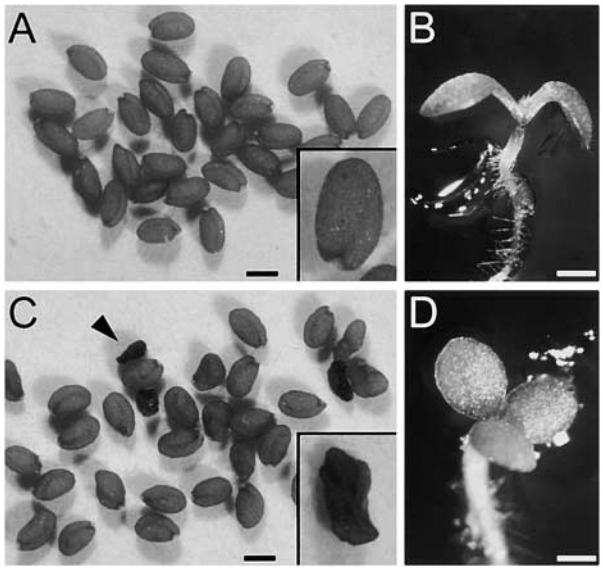

Figure 4. *sgr2* Seed and Seedlings.

(A) and **(C)** The mature seed in a >1.2-cm-long sheath. Typically shaped seed are shown magnified in the insets.
(A) Wild-type seed are uniformly oval.
(C) A few *sgr2* seed are abnormally shaped or shrunken (arrowhead).
(B) and **(D)** Seven- to 10-day-old seedlings.
(B) Wild-type seedling.
(D) A seedling with three cotyledons (*sgr2-1*).
Bars in **(A)** and **(C)** = 300 μm; bars in **(B)** and **(D)** = 1 mm.

Morphological Characterization of *zig*

The mutation of *ZIG* caused pleiotropic effects on the plant's morphology. The rosette leaves of the *zig* mutant were small and wrinkled. More remarkably, both the primary and lateral stems elongated in a zigzag fashion, bending at the nodes in the opposite direction to the cauline leaves or buds (Figure 2C). Their stems curved upward in the internodes. According to the metamer concept (Shultz and Haughn, 1991), Arabidopsis plants produce three types of metamer, with type 1, type 2, and type 3 metamers being rosette, coflorescence-bearing with cauline leaves, and flower-bearing without bract, respectively. Each metamer contains several nodes. In the wild-type plant, the angles formed by two adjoining internodes in the second and third metamer always were close to 180°, whereas in the *zig-1* mutant, the angles always were narrower (Table 1). In particular, in the mutant plant, the angles were narrower in the second metamer than in the third metamer, with those in the second metamer on the distal side from the rosette tending to be narrowest of all. Moreover, the length of the internodes in the second metamer was considerably shorter in *zig-1* than in the wild-type plant, particularly the proximal internodes (Table 2). There was no significant difference in the internode length in the third metamer.

To elucidate the cause of these morphological anomalies, the stem tissues were observed with an optical microscope. There were no aberrations in the structure of the shoot apical meristem and the location of peripheral primordia (data not shown). Furthermore, the patterning of the whole tissue was basically normal, although the cell shape and size were affected. In the mature *zig-1* stem, the epidermal cells were shorter and wider than those in the wild-type stem (Figures 7A and 7C). The size of the pith cells in the mutant stem varied, and their arrangement was disordered (Figures 7B and 7D). Thus, the zigzag-shaped stem of the *zig* mutant may be caused not by the abnormal positioning of the peripheral primordia but rather by the aberrant elongation, shape, and arrangement of cells. Aberrations in cell shape also were observed in other tissues of the mutant, including the pavement cells in leaves and trichomes and the epidermal cells in the hypocotyl (data not shown).

Map-Based Cloning of ZIG

We cloned the *ZIG* gene relative to its map position (Figure 8). We performed polymerase chain reaction (PCR)-based mapping of recombination breakpoints in 2422 chromosomes from F2 progeny. The position of the *ZIG* locus on chromosome 5 was narrowed to an ~380-kb region (Figure 8A). Because *zig-1* and *zig-2* were isolated from fast neutron–mutagenized lines, it was expected that the molecular lesions on the gene in these mutants would be deletions. To

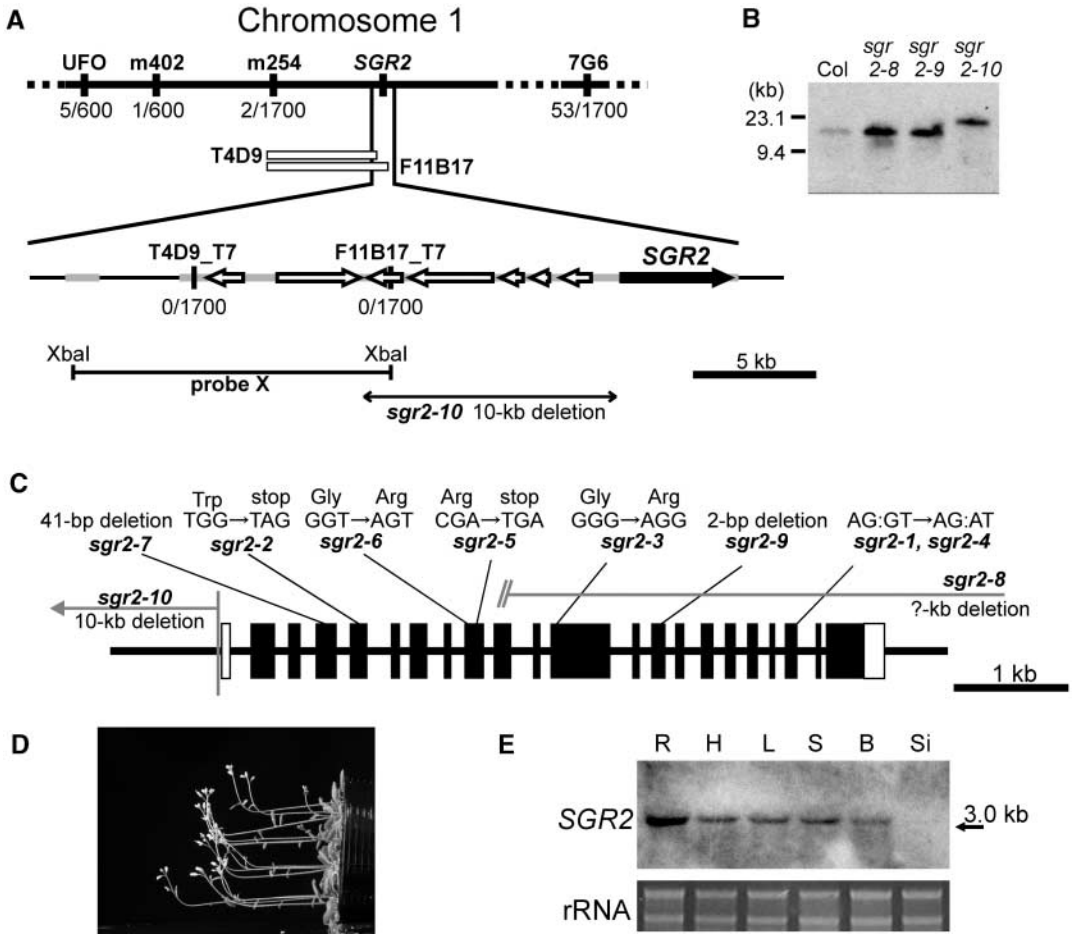

Figure 5. Molecular Cloning of the *SGR2* Gene

(A) *SGR2* was mapped to lie between the m254 and 7G6 markers on chromosome 1. The numbers of recombinants are indicated under these markers (recombinant chromosomes/analyzed chromosomes). Probe X (XbaI–XbaI fragment derived from F11B17) was used as a probe in DNA gel blot analysis.

(B) DNA gel blot analysis of three *sgr2* alleles that were generated by radiation mutagenization. These genomic DNAs, digested with XbaI, were loaded and blotted. A polymorphism was detected between *sgr2-10* and Col. Probe X DNA fragment was used as probe.

(C) The structure of the *SGR2* gene and the mutation sites of the *sgr2* alleles examined. Boxes represent exons: closed boxes, translated regions; open boxes, untranslated regions. *SGR2* is encoded by an ~5.8-kb genome fragment that contains 22 exons and 21 introns. Each mutation of 10 *sgr2* alleles is mapped in the genome region.

(D) Complementation of *sgr2* gravitropism by the wild-type *SGR2* genomic region.

(E) RNA gel blot analysis of *SGR2* mRNA levels in each wild-type organ. Each lane was loaded with 5 μg of total RNA. R, roots of a 7-day-old seedling; H, hypocotyl of an etiolated seedling grown in the dark for 3 days; L, mature rosette leaves; S, inflorescence stems; B, floral buds, including inflorescence meristem; Si, siliques.

detect the expected deletion, DNA gel blot analyses were performed on *zig-1* and *zig-2* using Mitsui P1 clones or transformation-competent artificial chromosome (TAC) clones as probes. When the TAC clone K16M23 was used as a probe, banding patterns that were different from those in the wild type were found simultaneously in *zig-1* and *zig-2* (data not shown). *zig-1* has a genomic discontinuity within the *MUL8.15* gene, according to the annotation in the Kazusa Arabidopsis data opening site (Figure 8B). The connection between the fifth intron of *MUL8.15* and the first intron of the putative *MPO12.P7* gene was detected in the *zig-1* mutants by thermal asymmetric interlaced PCR (Liu et al., 1995). This is consistent with the mapping results, which found no recombinants between MUL8 and MPO12. The in-

tervening region seemed to be present elsewhere in the genome, because the presence of the relevant region could be detected by DNA gel blot analysis. With respect to *zig-2*, an ~20-kb-long region of the chromosome that included the *MUL8.15* gene was deleted. In *zig-3*, a point mutation was found in the fifth exon of *MUL8.15*. This mutation is expected to result in the amino acid substitution of an Asp residue for the Gly-142 residue in a predicted coiled-coil domain (Figure 8C). The 5-kb wild-type genomic fragment containing *MUL8.15* was cloned and introduced into *zig-1* for a complementation test. The resulting transgenic plants showed wild-type morphology (Figure 8D), and their straight inflorescence stems responded normally to gravity (Figure 8E). These results indicate that *MUL8.15* is the authentic *ZIG* gene.

Surprisingly, this gene had been reported previously by Zheng et al. (1999) as *AtVTI1a*. It was identified as a homolog of the yeast v-SNARE *VTI1* by Arabidopsis EST database search. Yeast Vti1p is involved in multiple vesicle transport steps, including transport from the Golgi apparatus to vacuoles via endosomes (Holthuis et al., 1998; von Mollard and Stevens, 1999) and retrograde transport within the Golgi apparatus (Lupashin et al., 1997; von Mollard et al., 1997). Chromosomal rearrangement had occurred in *zig-1*, and abnormal transcripts were detected by RT-PCR (data not shown). Even if expressed, however, the putative product of the *zig-1* gene would be nonfunctional because it lacks the transmembrane domain and part of the coiled-coil region (Figure 8C). No transcripts were detected in *zig-2* by RT-PCR (data not shown). Thus, *zig-1* and *zig-2* can be regarded as null mutants. Because a highly conserved residue in the coiled-coil domain was substituted in *zig-3*, the mutant protein probably is reduced in its activity. The extent of the molecular lesion on each allele correlates well with the severity of its physiological (Figure 3B) and morphological (data not shown) phenotypes.

DISCUSSION

We have isolated a number of mutants whose shoots show a reduced gravitropic response. The genes involved in some mutants, namely, *SGR1*/*SCR* and *SGR7*/*SHR*, were cloned previously and appear to encode transcriptional factors that are essential in the formation of endodermis in both the shoot and the root (Di Laurenzio et al., 1996; Helariutta et al., 2000). This suggests that these two genes are not involved directly in the processes mediating the gravitropic response. Here we have characterized two other gravitropic mutants, *sgr2* and *zig*, and cloned the responsible genes. *sgr2* and *zig* both were abnormal in the gravitropic responses

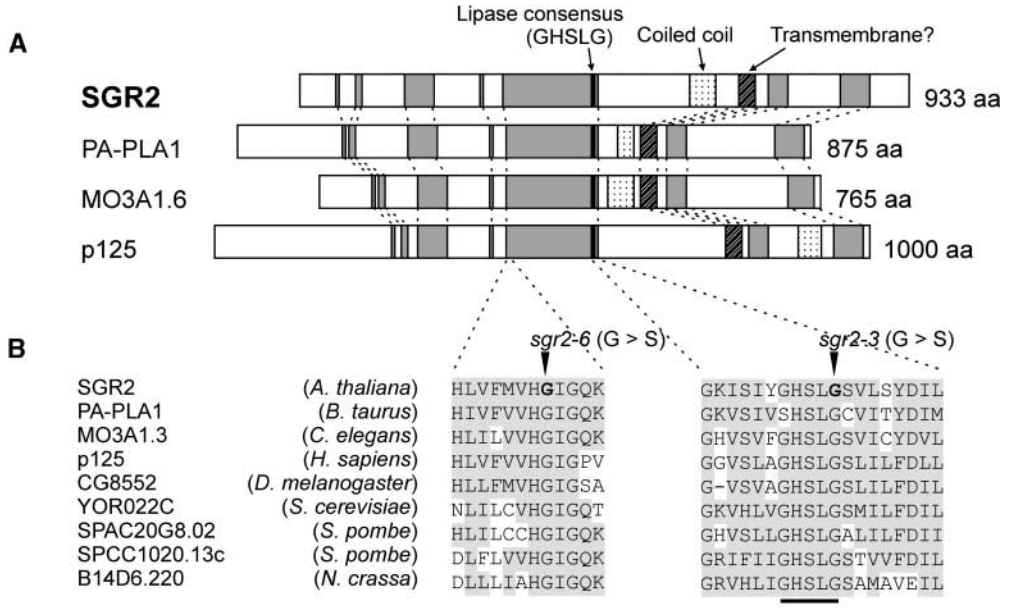

Figure 6. Structure of the SGR2 Protein and Its Homologs.

(A) Scheme of SGR2 (Arabidopsis), PA-PLA1 (*B. taurus*), MO3A1.6 (*C. elegans*), and p125 (*H. sapiens*). Boxes represent conserved sequences. aa, amino acids.

(B) Multiple sequence alignment of two regions that are conserved between SGR2 and its homologs. The horizontal line shows the lipase consensus sequence (GXSXG). Two boldface letters indicate the residues that are changed in *sgr2-3* and *sgr2-6*.

Table 1. Angles Forming at Nodes between Two Adjoining Internodes

	Wild Type (°)[a]	*zig* (°)[b]
Second metamer		
First node[c]	174.0 ± 1.1[d]	165.8 ± 2.6
Second node	178.3 ± 0.6	158.7 ± 2.7
Third node	176.8 ± 1.4	156.5 ± 2.1
Third metamer		
First node	177.1 ± 1.0	167.5 ± 1.4
Second node	178.4 ± 0.6	166.8 ± 1.8
Third node	177.1 ± 1.2	162.0 ± 1.3

The inflorescence stems were used after growth had been completed.
[a] $n = 12$.
[b] $n = 24$.
[c] The nodes were numbered from the proximal side of the rosette.
[d] 180° indicates a straight stem.

of their hypocotyls and inflorescence stems. Direct involvement of these genes in the gravitropic response is expected because mutant plants showed a normal radial pattern of the stem tissues. However, both mutants also exhibited morphological anomalies in organs that are not involved directly in the gravitropic response, suggesting that these genes probably play multiple roles in several organs.

SGR2 Is Similar in Sequence to PA-PLA1

The SGR2 exhibited sequence homology with the PA-PLA1 gene that was cloned from bovine testis. Genes that are similar to PA-PLA1 are found widely throughout the eukaryotes and form a gene family (Figure 6A). All members of this family contain a lipase consensus sequence (GXSXG) (Higgs et al., 1998), although PA-PLA1 is the only member to date actually shown to have lipase activity. Another gene that is relatively well characterized is the Sec23p-interacting protein, p125, that was identified in human (Tani et al., 1999). The biological functions of PA-PLA1 and p125 are unclear. Sequence searching predicts that all of the genes in the PA-PLA1 gene family are present in their respective genomes as single genes, at least in most organisms whose genome sequences are complete or nearly complete (such as *S. cerevisiae*, *C. elegans*, *D. melanogaster*, and Arabidopsis), except for *S. pombe*, which has two homologous genes. *SGR2* does not appear to be essential for viability because the *sgr2-7* and *sgr2-2* mutants still are viable in spite of severe molecular lesions that may result in the production of nonfunctional gene products (Figure 5C). Similarly, the YOR022c gene in *S. cerevisiae* also seems to be dispensable, because the YOR022c null mutant grew normally in glucose-rich medium (Winzeler et al., 1999). The dispensable nature of these genes might make it difficult to characterize their biological functions.

SGR2, like some other family members, was predicted to have a transmembrane domain (Figure 6A). Moreover, all members of the family have a highly conserved region homologous with a putative transmembrane domain present in the retinal degeneration B protein (Vihtelic et al., 1991, 1993). This finding suggests that the family members might encode membrane proteins.

It has been reported that the central serine (SHSLG) of the lipase consensus sequence is the active nucleophile, because the missense mutation of Ser to Ala in PA-PLA1 reduced its lipase activity (Higgs et al., 1998). When we produced recombinant SGR2 protein in *Escherichia coli* cells, we could not detect PLA1 activity (data not shown). This result might be attributable to aberrant protein folding or protein modification in *E. coli* cells. *sgr2-3*, which has little gravitropic response, has an amino acid substitution of Arg for the last Gly in the lipase consensus sequence (Figures 3A and 6B), suggesting that this conserved sequence is crucial for the function of SGR2.

If SGR2 has phospholipase activity, what could be the molecular function of SGR2 in the gravitropic response? Phospholipase A1 cleaves a phospholipid, a constituent of the membrane lipid bilayer, into a fatty acid and a lysophospholipid. It is conceivable that the degradation of specific phospholipids by phospholipases alters membrane composition and that this changes membrane structure, fluidity, or function. Although the sensing or signaling mechanism(s) involved in gravitropism remains obscure, physiological and electron microscopic analyses suggest that some membrane systems, such as endoplasmic reticulum and plasma membrane, may participate (Sack, 1997; Chen et al., 1999; Zheng and Staehelin, 2001). Thus, SGR2 may play a role in gravitropism by regulating such membrane systems. Alternatively, SGR2 may produce messenger molecule(s) by cleaving phospholipids. Plants possess many phospholipase families, and the functions of phospholipases A2, C,

Table 2. Length of the Internodes of the Inflorescence Stems

	Wild Type (mm)[a]	*zig* (mm)[b]
Second metamer		
First internode[c]	34.3 ± 4.7	8.0 ± 1.0
Second internode	35.3 ± 2.4	11.5 ± 1.0
Third internode	25.1 ± 1.4	13.7 ± 1.0
Third metamer		
First internode	20.0 ± 1.0	19.5 ± 0.8
Second internode	11.8 ± 0.8	9.5 ± 0.6
Third internode	11.6 ± 0.7	11.9 ± 0.5

The inflorescence stems were used after growth had been completed.
[a] $n = 26$.
[b] $n = 36$.
[c] The internodes were numbered from the proximal side of the rosette.

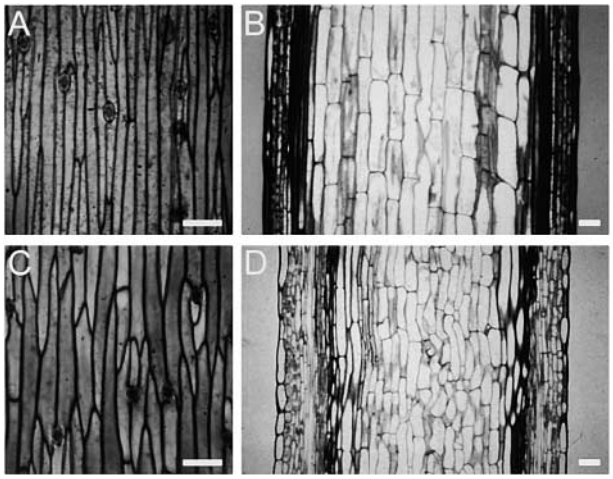

Figure 7. Histological Analysis of the *zig* Mutant.

(A) and **(C)** Epidermal cell layers of wild-type **(A)** and *zig-1* **(C)** inflorescence stems.
(B) and **(D)** Longitudinal sections of wild-type **(B)** and *zig-1* **(D)** inflorescence stems. Bars = 50 μm.

and D have been analyzed (Scherer and Arnold, 1997; Chapman, 1998; Wang, 1999). They are activated by internal or environmental stimuli and produce signal molecules that are associated with several physiological responses (Chapman, 1998). Although the involvement of phospholipase A1 in signal transduction pathways is poorly understood, even in animals, further investigation of SGR2 may extend our understanding of the role that phospholipase A1 plays in signal transduction.

One member of the PA-PLA1 family, p125, interacts with Sec23p, which mediates vesicle formation through a proline-rich N-terminal region of p125 (Tani et al., 1999; Mizoguchi et al., 2000). Although the other members, including SGR2, do not have such a proline-rich domain, they have putative coiled-coil domains and thus are expected to interact with other proteins. The amino acid sequences of these coiled-coil domains are not conserved. In addition, with respect to members of the PA-PLA1 gene family other than PA-PLA1, MO3A1.6, and SGR2, the positions of these regions in the protein are varied. Each family member may interact with various proteins. It is possible that the various members of the gene family share a common function as phospholipases but that their substrates or the manner in which their activity is regulated may differ.

ZIG/SGR4 Is a SNARE, AtVTI11

ZIG encodes a member of the SNARE class of proteins. SNAREs are key players in directing membrane fusion processes (McNew et al., 2000; Wickner and Haas, 2000). They can be divided into vesicle SNAREs (v-SNAREs, on vesicle membranes) and target SNAREs (t-SNAREs or syntaxins, on target membranes). The Arabidopsis Genome Initiative has not only confirmed the existence of orthologs of yeast SNAREs in Arabidopsis but also has revealed multiple paralogs and novel groups (Arabidopsis Genome Initiative, 2000; Sanderfoot et al., 2000). Some of these may play roles that are specific for higher plants. In fact, investigation of the mutant of the syntaxin-type SNARE gene *KNOLLE* showed this gene functions in cytokinesis (Lukowitz et al., 1996; Lauber et al., 1997). However, most of the SNARE disruption mutants examined so far are lethal; therefore, their specific functions have remained unknown (Sanderfoot et al., 2001).

We found that *ZIG* is identical to *AtVTI11*, which most likely is a v-SNARE and was cloned as a yeast *VTI1* homolog by an Arabidopsis EST database search by Zheng et al. (1999). Yeast Vti1p is involved in multiple vesicle transport pathways, such as transport from the Golgi apparatus to vacuoles via endosomes (Holthuis et al., 1998; von Mollard and Stevens, 1999) and retrograde transport within the Golgi apparatus (Lupashin et al., 1997; von Mollard et al., 1997). *ZIG*/*AtVTI11* is expressed in all Arabidopsis organs examined (data not shown). Immunoelectron microscopy has shown that ZIG/AtVTI11 is localized in the *trans*-Golgi network and the prevacuolar compartment (PVC) in Arabidopsis root cells (Zheng et al., 1999). ZIG/AtVTI11 can substitute for Vti1p in the Golgi-to-vacuole transport of carboxypeptidase Y in the yeast *vti1* temperature-sensitive mutant (Zheng et al., 1999). However, these studies have not clarified the precise function of *AtVTI11*, although it is supposed that *AtVTI11* is a housekeeping gene. In plants, there are two different types of vacuoles: lytic vacuoles and storage vacuoles. Storage vacuoles are unique to plants, and extensive studies have suggested that the molecular mechanism by which proteins are transported to plant lytic vacuoles may be more complex than that in yeast (Bassham and Raikhel, 2000). The PVC, which probably is a target for AtVTI11-containing vesicles, seems to mediate traffic to lytic vacuoles.

By characterizing the *zig* mutant, we have revealed novel function(s) of *ZIG*/*AtVTI11*. The *zig* mutant was morphologically anomalous and showed abnormal gravitropism in its hypocotyl and stem (Figures 1 and 5). These observations indicate that *ZIG* is involved in both the gravitropic response and plant morphogenesis and suggest that vesicle transport processes may be involved in gravitropism. It has been shown that ZIG/AtVTI11 interacts with the syntaxin homologs AtPEP12 and AtVAM3, which are localized in the PVC and the PVC/vacuole, respectively (Sato et al., 1997; Sanderfoot et al., 1999; Zheng et al., 1999). The mutant *zig-3*, whose gravitropic response is the most weakly affected of the three *zig* mutants, has an amino acid substitution in the conserved residue of the coiled-coil domain that is conserved in the *VTI1* family. This domain should be involved in

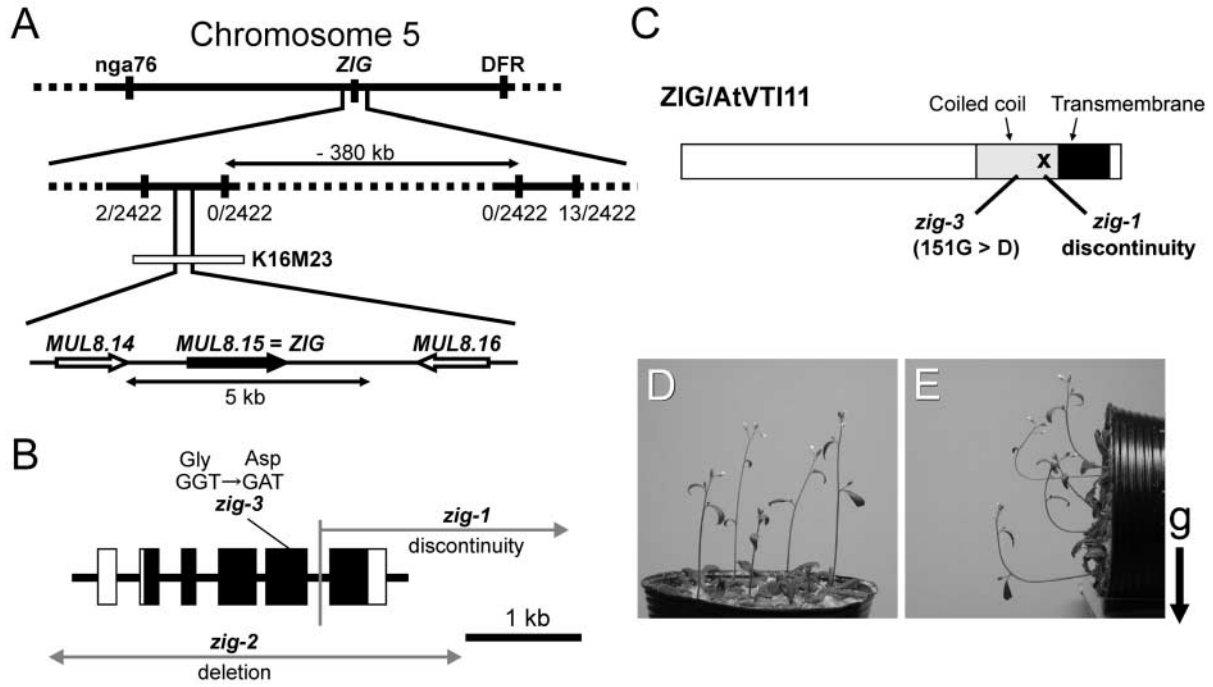

Figure 8. Molecular Cloning of the *ZIG* Gene.

(A) Initial mapping placed the *zig* mutation between the nga76 and DFR markers. Using newly generated PCR markers, the position of the *ZIG* locus was narrowed to an ~380-kb region. The numbers of recombinants among 2422 chromosomes tested are indicated (recombinant chromosomes/analyzed chromosomes). DNA gel blot analysis using the K16M23 TAC clone as a probe showed that deletions had occurred in both *zig-1* and *zig-2* in the region that contains *MUL8.15*.

(B) The structure of the *ZIG* gene and the mutation sites of the *zig* alleles examined. Boxes represent exons: closed boxes, translated regions; open boxes, untranslated regions. *zig-2* had lost the *ZIG* gene completely as well as some neighboring genes (data not shown).

(C) Molecular lesion in each allele shown on the protein. The X shows the chromosomal discontinuity in *zig-1*. Black and gray boxes indicate a predicted transmembrane domain and a coiled-coil domain, respectively, of ZIG/AtVTI11.

(D) and **(E)** Complementation of *zig* by the wild-type *ZIG* genomic region. The 5-kb genomic DNA fragment that includes *MUL8.15* **(A)** was transformed into *zig-1* plants.

(D) The resulting 4-week-old transgenic plants.

(E) Plants placed horizontally for 2 hr at 23°C in the dark. The arrow indicates the direction of gravity (g).

interaction with a partner SNARE, and this interaction may decrease in *zig-3*. It is conceivable that it is the cargo transported by the ZIG-dependent pathway, rather than ZIG itself, that is required for gravitropism or morphogenesis. Notably, although the disruption of *VTI1* is lethal in yeast (von Mollard and Stevens, 1999), *ZIG* is dispensable in Arabidopsis. Because Arabidopsis has three *VTI1* homologs (Arabidopsis Genome Initiative, 2000; Sanderfoot et al., 2000), they may be redundant, at least for the vital role(s) they mediate.

How Do SGR2 and ZIG Relate to Each Other?

Because SGR2 was predicted to have a transmembrane domain, it is expected to localize to a certain membrane compartment, although it does not appear to contain localization signals that would direct it to particular organelles. Interestingly, the cells of some *sgr2* embryos have been observed to have abnormal membrane structures (T. Kato and M. Tasaka, unpublished data). Such abnormalities may be responsible for the aberrant morphology seen in some *sgr2* mutant seedlings. In addition, it has been reported that phospholipase A1 activity was detected in the vacuole membrane fraction of *Acer pseudoplatanus* cultured cells (Tavernier and Pugin, 1995). With regard to ZIG, the functional complementation of ZIG/AtVTI11 in yeast and the subcellular localization and molecular interactions of this protein in root cells of Arabidopsis suggest that ZIG is involved in vesicle transport to vacuoles, probably via the PVCs (Zheng et al., 1999). Together, these observations suggest that both SGR2 and ZIG participate in vacuole function. In the accompanying paper, the involvement of SGR2 and ZIG in vacuolar functions is investigated.

METHODS

Plant Materials and Growth Conditions

The Columbia (Col) and Wassilewskija (Ws) ecotypes of *Arabidopsis thaliana* were used as the wild type. *sgr2-1*, *-2*, *-3*, *-4*, *-5*, and *-6* were isolated from the M2 population of Col that had been mutagenized by ethyl methanesulfonate. *sgr2-7* was isolated from T-DNA insertion Ws lines (DuPont) (Fukaki et al., 1996b). *sgr2-8*, *sgr2-9*, and *sgr2-10* were isolated from the M2 population of Col mutagenized by fast neutron exposure (Lehle Seeds, Round Rock, TX). *zig-1*/*sgr4-1* was isolated from fast neutron–mutagenized Col seed lots, as described previously (Yamauchi et al., 1997). *zig-2* and *zig-3* were newly isolated from fast neutron–mutagenized Col seed and T-DNA insertion Ws lines (DuPont), respectively. The screening strategy used to isolate these mutants has been described (Fukaki et al., 1996b), and their allelism was confirmed by being crossed with each other. Plants were grown in soil under constant white light at 23°C and used to assay the gravitropism of their inflorescence stems. Three-day-etiolated seedlings grown on Murashige and Skoog (1962) medium at 23°C also were analyzed as described previously (Fukaki et al., 1996a, 1996b). Approximately 700 seed from 10 siliques were plated on Murashige and Skoog plates and incubated under constant white light at 23°C to analyze the phenotype of the *sgr2* seedlings.

Gravitropism Assay

To examine the gravitropic responses of inflorescence stems, intact plants or segments of young primary stems 4 to 8 cm in length were used. The 4-cm-long stem segments included shoot apices and all lateral organs. The stem segments were preincubated in a vertical orientation under light at 23°C and then placed horizontally in darkness at 23°C, as described previously (Fukaki et al., 1996a). To measure the gravitropic response of intact stems, vinyl pots in which the plants were grown were placed horizontally in darkness at 23°C. The curvature of the stem was measured as the angle formed between the growing direction of the apex and the horizontal baseline. At least 20 individuals of each genotype were examined.

Histological Analysis

Stem segments were cut from primary inflorescence stems that grew upright after bolting and fixed in 10% (v/v) formaldehyde, 5% (v/v) acetic acid, and 50% (v/v) ethanol in 0.2-mL tubes under vacuum. After fixation, samples were dehydrated by a series of ethanol washes and embedded in Technovit 7100 (Heraeus Kulzer, Wehrheim, Germany) according to the manufacturer's instructions. Sections (3 μm) were stained with toluidine blue. Epidermal cell layers were peeled from the inflorescence stems and then stained with toluidine blue.

Mapping and Cloning of the *SGR2* Gene

The *sgr2-1* mutation was mapped to lie between the UFO (UNUSUAL FLORAL ORGANS) cleaved-amplified polymorphic sequence marker (5 recombinants) and the *tt1* genetic marker (35 recombinants) on chromosome 1 after analysis of 600 chromosomes. One of five recombinants in the UFO-*sgr2* region had a recombination point in the m402 restriction fragment length polymorphism marker *sgr2*. A bacterial artificial chromosome (BAC) and transformation-competent artificial chromosome (TAC) contig between UFO and m254 was constructed. A TAC library (Liu et al., 1999) was screened using various DNA probes (UFO, m402, and m254), and BAC clones were selected on the basis of World Wide Web–derived information on BAC end sequences and BAC hybridization data on yeast artificial chromosome (YAC) and BAC fingerprints. Some polymerase chain reaction (PCR) markers were synthesized on the basis of the end sequences of the clones obtained. Additional fine analysis of 1100 chromosomes (total, 1700 chromosomes) was performed. *sgr2* was mapped initially between the AtSO392 simple sequence length polymorphism marker (42 recombinants) and the T27K12-SP6 simple sequence length polymorphism marker (116 recombinants).

DNA gel blot analysis was performed to determine the polymorphism between the wild-type and the fast neutron–mutagenized *sgr2-8*, *sgr2-9*, and *sgr2-10* genomic DNA. Thus, 2 μg of genomic DNA was digested with eight restriction enzymes: XbaI, HindIII, BglI, DraIII, EcoRI, EcoRV, KpnI, and PstI (data not shown). The >10-kb XbaI fragment (Figure 5A, probe X) digested from BAC F11B17 was used as a probe. Hybridization and signal detection were performed with the ECL Direct System (Amersham Pharmacia Biotech).

The 26-kb genomic DNA region, including both sides of the XbaI fragment, was sequenced. Eight putative genes were identified in the genome using the BLAST search and the annotation of the Arabidopsis Genome Initiative. By sequencing each putative coding region, each mutation of all 10 *sgr2* alleles was mapped to one gene. 5′- and 3′-rapid amplification of cDNA ends kits from Life Technologies (Grand Island, NY) defined the coding region. A 7.3-kb BamHI–ClaI fragment that included the 1.2-kb upstream region of the gene and the 500-bp downstream region was cloned into pBIN19. The clone was introduced into *Agrobacterium tumefaciens* strain MP90 and transformed into the *sgr2-1* plants by the floral dip method (Clough and Bent, 1998).

Mapping and Cloning of the *ZIG* Gene

The *zig-1* homozygous mutant was crossed to Landsberg *erecta* wild-type plants to generate a mapping population. Approximately 50 recombinants of the F2 progeny were screened for the *zig-1* phenotype for rough mapping. The position of *ZIG* was located in the middle of chromosome 5. For fine scale mapping, DNA was prepared from 1211 F2 progeny. Polymorphism between Col and Landsberg *erecta* were identified, which allowed PCR markers to be designed based on the chromosome 5 sequence data from the Arabidopsis Genome Initiative supplied by the Kazusa group. The resulting cleaved-amplified polymorphic sequence markers were used to map the recombination breakpoints by PCR and restriction digestion.

The 5.0-kb genomic DNA fragment from TAC clone K16M23 (Liu et al., 1999) was cloned into binary vector pBIN19. The construct (pBINgZIG) was transformed into *A. tumefaciens* strain MP90 and then introduced into the *zig-1* plants (Clough and Bent, 1998). T1 plants were selected by resistance to kanamycin and stem shape. The presence of the transgene in these plants was tested by PCR. Segregation of the transgene in the T2 generation was confirmed.

RNA Gel Blot Analysis

For RNA gel blot analysis, total RNA was isolated according to methods using aurintricarboxylic acid. Subsequently, 5 μg of total of RNA was electrophoresed on a 1% agarose gel containing 2.2 M formaldehyde and transferred to a nylon membrane (Hybond-N^+; Amersham Pharmacia Biotech). The 700-bp *SGR2* cDNA fragment amplified by PCR with primers 5′-GATTTTGCTGCACGTTCACAG-3′ and 5′-ACTGGATCCTACTTCTGCACAGG-3′ was cloned into pGEM-T Vector (Promega) and used as a template for RNA probes. Blots were hybridized overnight at 23°C in the hybridization buffer containing 1 μg/mL digoxigenin-labeled RNA probe. Immunological detection was performed according to the manufacturer's instructions. Chemiluminescence was performed with CDP-Star (Boehringer Mannheim) and exposed to Hyperfilm MP (Amersham Pharmacia Biotech).

Accession Numbers

The GenBank accession numbers for *SGR2* and *ZIG* are AB073133 and AF114750, respectively.

ACKNOWLEDGMENTS

We thank Dr. Hisao Fujisawa and Dr. Akihiko Nakano for helpful discussions, the Arabidopsis Biological Resource Center (Ohio State University, Columbus) for providing seed and BAC clones, the Kazusa DNA Research Institute for providing TAC and Mitsui P1 clones, and the Arabidopsis Genome Initiative for Arabidopsis genome projects. This work was supported in part by the Ministry of Agriculture, Forestry, and Fisheries of Japan in the framework of the Pioneering Research Project in Biotechnology.

Received May 29, 2001; accepted September 26, 2001.

REFERENCES

Arabidopsis Genome Initiative. (2000). Analysis of the genome sequence of the flowering plant *Arabidopsis thaliana*. Nature **408,** 796–815.

Bassham, D.C., and Raikhel, N.V. (2000). Plant cells are not just green yeast. Plant Physiol. **122,** 999–1001.

Belyavskaya, N.A. (1996). Calcium and graviperception in plants: Inhibitor analysis. Int. Rev. Cytol. **168,** 123–185.

Bennett, M.J., Marchant, A., Green, H.G., May, S.T., Ward, S.P., Millner, P.A., Walker, A.R., Schulz, B., and Feldmann, K.A. (1996). *Arabidopsis AUX1* gene: A permease-like regulator of root gravitropism. Science **273,** 948–950.

Chapman, K.D. (1998). Phospholipase activity during plant growth and development and in response to environmental stress. Trends Plant Sci. **3,** 419–426.

Chen, R., Hilson, P., Sedbrook, J., Rosen, E., Caspar, T., and Masson, P.H. (1998). The *Arabidopsis thaliana AGRAVITROPIC 1* gene encodes a component of the polar-auxin-transport efflux carrier. Proc. Natl. Acad. Sci. USA **95,** 15112–15117.

Chen, R., Rosen, E., and Masson, P.H. (1999). Gravitropism in higher plants. Plant Physiol. **120,** 343–350.

Clough, S.J., and Bent, A.F. (1998). Floral dip: A simplified method for *Agrobacterium*-mediated transformation of *Arabidopsis thaliana*. Plant J. **16,** 735–743.

Di Laurenzio, L., Wysocka-Diller, J., Malamy, J.E., Pysh, L., Helariutta, Y., Freshour, G., Hahn, M.G., Feldmann, K.A., and Benfey, P.N. (1996). The *SCARECROW* gene regulates an asymmetric cell division that is essential for generating the radial organization of the Arabidopsis root. Cell **86,** 423–433.

Fasano, J.M., Swanson, S.J., Blancaflor, E.B., Dowd, P.E., Kao, T., and Gilroy, S. (2001). Changes in root cap pH are required for the gravity response of the Arabidopsis root. Plant Cell **13,** 907–922.

Firn, R.D., Wagstaff, C., and Digby, J. (2000). The use of mutants to probe models of gravitropism. J. Exp. Bot. **51,** 1323–1340.

Fukaki, H., Fujisawa, H., and Tasaka, M. (1996a). Gravitropic response of inflorescence stems in *Arabidopsis thaliana*. Plant Physiol. **110,** 933–943.

Fukaki, H., Fujisawa, H., and Tasaka, M. (1996b). *SGR1*, *SGR2*, *SGR3*: Novel genetic loci involved in shoot gravitropism in *Arabidopsis thaliana*. Plant Physiol. **110,** 945–955.

Fukaki, H., Fujisawa, H., and Tasaka, M. (1997). The *RHG* gene is involved in root and hypocotyl gravitropism in *Arabidopsis thaliana*. Plant Cell Physiol. **38,** 804–810.

Fukaki, H., Wysocka-Diller, J., Kato, T., Fujisawa, H., Benfey, P.N., and Tasaka, M. (1998). Genetic evidence that the endodermis is essential for shoot gravitropism in *Arabidopsis thaliana*. Plant J. **14,** 425–430.

Fukaki, H., Tameda, S., Masuda, H., and Tasaka, M. (2002). Lateral root formation is blocked by a gain-of-function mutation in the *SOLITARY-ROOT/IAA14* gene of *Arabidopsis*. Plant J. **29,** in press.

Harper, R.M., Stowe-Evans, E.L., Luesse, D.R., Muto, H., Tatematsu, K., Watahiki, M.K., Yamamoto, K., and Liscum, E. (2000). The *NPH4* locus encodes the auxin response factor ARF7, a conditional regulator of differential growth in aerial Arabidopsis tissue. Plant Cell **12,** 757–770.

Helariutta, Y., Fukaki, H., Wysocka-Diller, J., Nakajima, K., Jung, J., Sena, G., Hauser, M.T., and Benfey, P.N. (2000). The *SHORT-ROOT* gene controls radial patterning of the Arabidopsis root through radial signaling. Cell **101,** 555–567.

Higgs, H.N., Han, M.H., Johnson, G.E., and Glomset, J.A. (1998). Cloning of a phosphatidic acid-preferring phospholipase A1 from bovine testis. J. Biol. Chem. **273,** 5468–5477.

Hofmann, K., and Stoffel, W. (1993). TMbase—A database of membrane spanning proteins segments. Biol. Chem. Hoppe-Seyler. **374,** 166.

Holthuis, J.C.M., Nichols, B.J., Dhruvakumar, S., and Pelham, H.R.B. (1998). Two syntaxin homologues in the TGN/endosomal system of yeast. EMBO J **17,** 113–126.

Kaufman, P.B., Wu, L., Brock, T.G., and Kim, D. (1995). Hormones and the orientation of growth. In Plant Hormones, P.J. Davies, ed

(Dordrecht, The Netherlands: Kluwer Academic Publishers), pp. 547–571.

Lauber, M.H., Waizenegger, I., Steinmann, T., Schwarz, H., Mayer, U., Hwang, I., Lukowitz, W., and Jürgens, G. (1997). The *Arabidopsis* KNOLLE protein is a cytokinesis-specific syntaxin. J. Cell Biol. **139,** 1485–1493.

Leyser, H.M.O., Lincoln, C.A., Timpte, C., Lammer, D., Turner, J., and Estelle, M. (1993). *Arabidopsis* auxin-resistance gene *AXR1* encodes a protein related to ubiquitin-activating enzyme E1. Nature **364,** 161–164.

Liscum, E., and Briggs, W.R. (1996). Mutations of Arabidopsis in potential transduction and response components of the phototropic signaling pathway. Plant Physiol. **112,** 291–296.

Liu, Y.G., Mitsukawa, N., Oosumi, T., and Whittier, R.F. (1995). Efficient isolation and mapping of *Arabidopsis thaliana* T-DNA insert junctions by thermal asymmetric interlaced PCR. Plant J. **8,** 457–463.

Liu, Y.-G., Shirano, Y., Fukaki, H., Yanai, Y., Tasaka, M., Tabata, S., and Shibata, D. (1999). Complementation of plant mutants with large genomic DNA fragments by a transformation-competent artificial chromosome vector accelerates positional cloning. Proc. Natl. Acad. Sci. USA **96,** 6535–6540.

Lukowitz, W., Mayer, U., and Jürgens, G. (1996). Cytokinesis in the Arabidopsis embryo involves the syntaxin-related KNOLLE gene product. Cell **84,** 61–71.

Lupas, A., Van Dyke, M., and Stock, J. (1991). Predicting coiled coils from protein sequences. Science **252,** 1162–1164.

Lupashin, V.V., Pokrovskaya, I.D., McNew, J.A., and Waters, M.G. (1997). Characterization of a novel yeast SNARE protein implicated in Golgi retrograde traffic. Mol. Biol. Cell **8,** 2659–2676.

Luschnig, C., Gaxiola, R.A., Grisafi, P., and Fink, G.R. (1998). *EIR1*, a root-specific protein involved in auxin transport, is required for gravitropism in *Arabidopsis thaliana*. Genes Dev. **12,** 2175–2187.

McNew, J.A., Parlati, F., Fukuda, R., Johnston, R.J., Paz, K., Paumet, F., Söllner, T.H., and Rothman, J.E. (2000). Compartmental specificity of cellular membrane fusion encoded in SNARE proteins. Nature **407,** 153–159.

Mizoguchi, T., Nakajima, K., Hatsuzawa, K., Nagahama, M., Hauri, H.-P., Tagaya, M., and Tani, K. (2000). Determination of functional regions of p125, a novel mammalian Sec23p-interacting protein. Biochem. Biophys. Res. Commun. **279,** 144–149.

Müller, A., Guan, C., Gälweiler, L., Tänzler, P., Huijser, P., Marchant, A., Parry, G., Bennett, M., Wisman, E., and Palme, K. (1998). *AtPIN2* defines a locus of *Arabidopsis* for root gravitropism control. EMBO J. **17,** 6903–6911.

Murashige, T., and Skoog, F. (1962). A revised medium for rapid growth and bioassays with tobacco tissue culture. Physiol. Plant. **15,** 473–497.

Nagpal, P., Walker, L.M., Young, J.C., Sonawala, A., Timpte, C., Estelle, M., and Reed, J.W. (2000). *AXR2* encodes a member of the Aux/IAA protein family. Plant Physiol. **123,** 563–574.

Perera, I.Y., Heilmann, I., and Boss, W.F. (1999). Transient and sustained increases in inositol 1,4,5-trisphosphate precede the differential growth response in gravistimulated maize pulvini. Proc. Natl. Acad. Sci. USA **96,** 5838–5843.

Rouse, D., Mackay, P., Stirnberg, P., Estelle, M., and Leyser, O. (1998). Changes in auxin response from mutations in an *AUX/IAA* gene. Science **279,** 1371–1373.

Sack, F.D. (1991). Plant gravity sensing. Int. Rev. Cytol. **127,** 193–252.

Sack, F.D. (1997). Plastids and gravitropic sensing. Planta **203,** S63–S68.

Sanderfoot, A.A., Kovaleva, V., Zheng, H., and Raikhel, N.V. (1999). The t-SNARE AtVAM3p resides on the prevacuolar compartment in *Arabidopsis* root cells. Plant Physiol. **121,** 929–938.

Sanderfoot, A.A., Assaad, F.F., and Raikhel, N.V. (2000). The Arabidopsis genome: An abundance of soluble *N*-ethylmaleimide-sensitive factor adaptor protein receptors. Plant Physiol. **124,** 1558–1569.

Sanderfoot, A.A., Pilgrim, M., Adam, L., and Raikhel, N.V. (2001). Disruption of individual members of Arabidopsis syntaxin gene families indicates each has essential functions. Plant Cell **13,** 659–666.

Sato, M.H., Nakamura, N., Ohsumi, Y., Kouchi, H., Kondo, M., Hara-Nishimura, I., Nishimura, M., and Wada, Y. (1997). The *AtVAM3* encodes a syntaxin-related molecule implicated in the vacuolar assembly in *Arabidopsis thaliana*. J. Biol. Chem. **272,** 24530–24535.

Scherer, G.F.E., and Arnold, B. (1997). Inhibitors of animal phospholipase A2 enzymes are selective inhibitors of auxin-dependent growth: Implications for auxin-induced signal transduction. Plant J. **16,** 462–469.

Scheres, B., Di Laurenzio, L., Willemsen, V., Hauser, M.-T., Janmaat, K., Weisbeek, P., and Benfey, P.N. (1995). Mutations affecting the radial organisation of the *Arabidopsis* root display specific defects throughout the embryonic axis. Development **121,** 53–62.

Scott, A.C., and Allen, N.S. (1999). Changes in cytosolic pH within Arabidopsis root columella cells play a key role in the early signaling pathway for root gravitropism. Plant Physiol. **121,** 1291–1298.

Sedbrook, J.C., Chen, R., and Masson, P.H. (1999). *ARG1* (altered response to gravity) encodes a DnaJ-like protein that potentially interacts with the cytoskeleton. Proc. Natl. Acad. Sci. USA **96,** 1140–1145.

Shultz, E.A., and Haughn, G.W. (1991). *LEAFY*, a homeotic gene that regulates inflorescence development in Arabidopsis. Plant Cell **3,** 771–781.

Sinclair, W., and Trewavas, A.J. (1997). Calcium in gravitropism: A re-examination. Planta **203,** S85–S90.

Tani, K., Mizoguchi, T., Iwamatsu, A., Hatsuzawa, K., and Tagaya, M. (1999). p125 is a novel mammalian Sec23p-interacting protein with structural similarity to phospholipid-modifying proteins. J. Biol. Chem. **274,** 20505–20512.

Tasaka, M., Kato, T., and Fukaki, H. (2001). Genetic regulation of gravitropism in higher plants. Int. Rev. Cytol. **206,** 135–154.

Tavernier, E., and Pugin, A. (1995). Phospholipase activities associated with the tonoplast from *Acer pseudoplatanus* cells: Identification of a phospholipase A1 activity. Biochim. Biophys. Acta **1233,** 118–122.

Tian, Q., and Reed, J.W. (1999). Control of auxin-regulated root development by the *Arabidopsis thaliana SHY2/IAA3* gene. Development **126,** 711–721.

Timpte, C.S., Wilson, A.K., and Estelle, M. (1992). Effects of the *axr2* mutation of *Arabidopsis* on cell shape in hypocotyl and inflorescence. Planta **188,** 271–278.

Utsuno, K., Shikanai, T., Yamada, Y., and Hashimoto, T. (1998). *AGR*, an *agravitropic* locus of *Arabidopsis thaliana*, encodes a novel membrane-protein family member. Plant Cell Physiol. **39,** 1111–1118.

Vihtelic, T.S., Hyde, D.R., and O'Tousa, J.E. (1991). Isolation and characterization of the Drosophila *retinal degeneration B* (*rdgB*) gene. Genetics **127,** 761–768.

Vihtelic, T.S., Goebl, M., Milligan, S., O'Tousa, J.E., and Hyde, D.R. (1993). Localization of *Drosophila retinal degeneration B*, a membrane-associated phosphatidylinositol transfer protein. J. Cell Biol. **122,** 1013–1022.

von Mollard, G.F., Nothwehr, S.F., and Stevens, T.H. (1997). The yeast v-SNARE Vti1p mediates two vesicle transport pathways through interactions with the t-SNAREs Sed5p and Pep12p. J. Cell Biol. **137,** 1511–1524.

von Mollard, G.F., and Stevens, T.H. (1999). The *Saccharomyces cerevisiae* v-SNARE Vti1p is required for multiple membrane transport pathways to the vacuole. Mol. Biol. Cell **10,** 1719–1732.

Wang, X. (1999). The role of phospholipase D in signaling cascades. Plant Physiol. **120,** 645–651.

Watahiki, M.K., and Yamamoto, K.T. (1997). The *massugu1* mutation of Arabidopsis identified with failure of auxin-induced growth curvature of hypocotyl confers auxin insensitivity to hypocotyl and leaf. Plant Physiol. **115,** 419–426.

Wickner, W., and Haas, A. (2000). Yeast homotypic vacuole fusion: A window on organelle trafficking mechanisms. Annu. Rev. Biochem. **69,** 247–275.

Wilson, A.K., Pickett, F.B., Turner, J.C., and Estelle, M. (1990). A dominant mutation in *Arabidopsis* confers resistance to auxin, ethylene and abscisic acid. Mol. Gen. Genet. **222,** 377–383.

Winzeler, E.A., et al. (1999). Functional characterization of the *S. cerevisiae* genome by gene deletion and parallel analysis. Science **285,** 901–906.

Yamauchi, Y., Fukaki, H., Fujisawa, H., and Tasaka, M. (1997). Mutations in the *SGR4*, *SGR5* and *SGR6* loci of *Arabidopsis thaliana* alter the shoot gravitropism. Plant Cell Physiol. **38,** 530–535.

Zheng, H., von Mollard, G.F., Kovaleva, V., Stevens, T.H., and Raikhel, N.V. (1999). The plant vesicle-associated SNARE AtVTI1a likely mediates vesicle transport from the *trans*-Golgi network to the prevacuolar compartment. Mol. Biol. Cell **10,** 2251–2264.

Zheng, H.Q., and Staehelin, L.A. (2001). Nodal endoplasmic reticulum, a specialized form of endoplasmic reticulum found in gravity-sensing root tip columella cells. Plant Physiol. **125,** 252–265.